International Journal of Mass Spectrometry 287 (2009) 87–95

Contents lists available at ScienceDirect

International Journal of Mass Spectrometry

journal homepage: www.elsevier.com/locate/ijms

Gas-phase hydrogen/deuterium exchange of dinucleotides and 5′-monophosphate dinucleotides in a quadrupole ion trap

Joseph E. Chipuk, Jennifer S. Brodbelt*

Department of Chemistry and Biochemistry, University of Texas at Austin, 1 University Station A5300, Austin, TX 78712, United States

ARTICLE INFO

Article history:
Received 28 June 2008
Received in revised form
21 September 2008
Accepted 23 September 2008
Available online 2 October 2008

Keywords:
H/D exchange
Dinucleotides
Relay mechanism

ABSTRACT

Gas-phase hydrogen/deuterium (H/D) exchange reactions of four deprotonated dinucleotides (dAA, dAG, dGA, dGG) and their 5′-monophosphate analogs (5′-dAA, 5′-dAG, 5′-dGA, 5′-dGG) with D_2O were performed in a quadrupole ion trap mass spectrometer. Significant differences in the rates and extents of exchange were found when the 5′-hydroxyl group of the dinucleotides was replaced by a phosphate functionality. Extensive and nucleobase-dependent exchange occurred for the deprotonated 5′-monophosphate dinucleotides, whereas the dinucleotides all exhibited essentially the same limited exchange. Results for the isomeric 5′-monophosphates, 5′-dAG and 5′-dGA, were remarkably different, indicating that the H/D exchange reaction was sequence dependent. An elaborate array of computations was performed to investigate the gas-phase structures of the ions individually and also as participants in ion-molecule complexes with D_2O. Integration of the experimental and theoretical results supports a relay exchange mechanism and suggests that the exchange behavior depends highly on the identity and sequence of the nucleobases as well as their ability to interact with the deprotonation site. Finally, a shuttling mechanism is proposed to possibly account for the bimodal H/D exchange behavior observed for deprotonated 5′P-dGA. In this case, hydrogen bonding between the nucleobases in concert with interaction from the deuterating agent creates an ion-molecule complex in which hydrogen and deuterium atoms may be shuttled amongst the hydrogen-bonded participants.

1. Introduction

Gas-phase hydrogen/deuterium (H/D) exchange reactions have become an increasingly important method for characterizing the gas-phase conformations of ions [1–29]. In recent years, these studies have been augmented by extensive molecular modeling in an effort to provide further support for mechanistic and structural details of the H/D exchange reactions of small organic molecules [1–3,6,8,9,14,17,24], as well as affording incredible insight into the gas-phase conformations of biological molecules, such as proteins and DNA [11,20,25,28,29,30]. The gas-phase structures of mononucleotides and dinucleotides [4,5,12,13,15,23], in addition to some large oligonucleotides [7,11,20,25,27], have been examined by H/D exchange methods in a number of studies using different deuterating reagents and types of mass spectrometers.

Past studies of H/D exchange of both 5′- and 3′-mononucleotides showed that the extents and rates of exchange varied with both the nucleobase and position of the terminal phosphate group [4,5,23] and required favorable spatial proximity between the phosphate group and the nucleobase [12]. Several 5′-phosphate mononucleotides completely exchanged their labile hydrogen atoms while reactions involving the corresponding 3′-phosphate isomers resulted in the incorporation of only two deuteriums, a result that correlated with whether the nucleobase was involved in the H/D exchange or was accessible to the deprotonated phosphate in either of the ribose positions [23].

Gas-phase H/D exchange experiments [26,27] and ion mobility measurements of dinucleotides have also been reported [31,32]. The ion mobility studies concluded that multiple gas-phase conformations of similar energy existed and that the conformations were both nucleobase- and sequence-dependent. Ion-molecule reaction studies conducted in an FT-ICR mass spectrometer revealed that the H/D exchange rates of selected dinucleotides with deuterated methanol were dependent on the nucleobase composition; however, no isomers were studied and hence no relationship with nucleobase sequence was established. H/D exchange of several isomeric pentanucleotides [7] and the hexanucleotide C_6 [27] also suggested that multiple gas-phase conformations of oligonucleotides existed and that these conformations exchanged at different rates, with bimodal distributions of exchange products observed at longer exchange times.

* Corresponding author. Tel.: +1 512 471 0028.
E-mail address: jbrodbelt@mail.utexas.edu (J.S. Brodbelt).

1387-3806/$ – see front matter © 2008 Elsevier B.V. All rights reserved.
doi:10.1016/j.ijms.2008.09.011

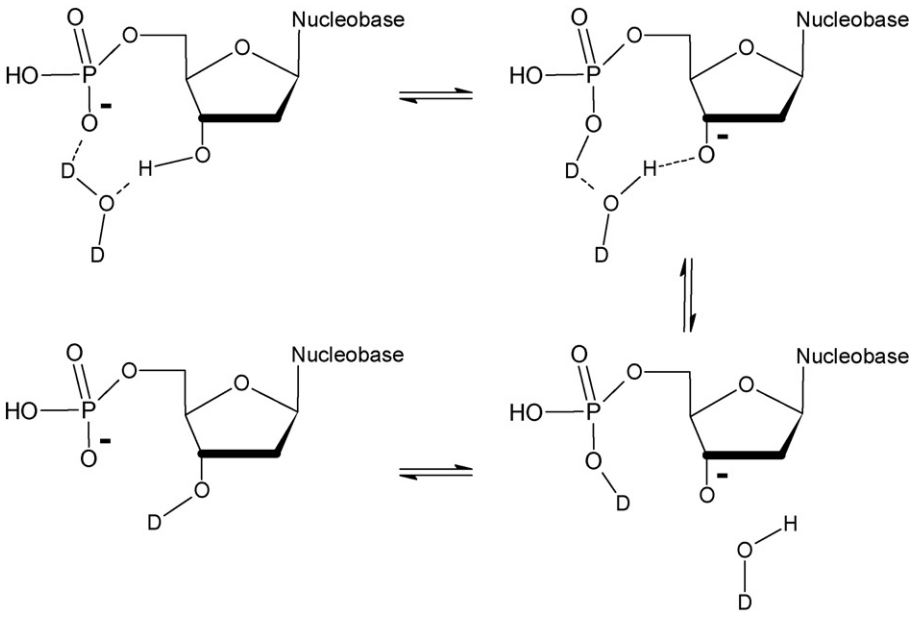

Scheme 1. H/D exchange via the relay mechanism. The reaction is shown for a generic mononucleotide, but the mechanism remains the same for any deprotonated phosphate and labile hydrogen atom.

Previous studies by several groups have suggested that H/D exchange of mononucleotides proceeds via a relay mechanism [4,5,12,23] (Scheme 1). In this mechanism, a stable ion-molecule complex is formed in which a deuterating reagent bridges the gap between a charge site and a labile hydrogen atom, thereby allowing indirect interaction of the two remote sites. For anions, the charge site serves as the deuterium acceptor in the exchange process, while the labile hydrogen atom is transferred to the deuterating agent. Recent reports suggest that dinucleotide exchange cannot be explained entirely by a relay mechanism [26]. Instead, a novel kinetic mechanism that is independent of the charge site but dependent on the relative time each exchangeable hydrogen atom is protected from the deuterating agent is proposed. These results are compelling and have provided new insight into the potential mechanisms of gas-phase H/D exchange.

Our exploration of the H/D exchange of oligonucleotides, and by association their gas-phase conformations, is continued in this work. In this case, a subset of the dinucleotides containing only purine nucleobases along with the analogous series of 5′-monophosphate dinucleotides is targeted (Fig. 1). Based on the comparison of the H/D exchange results of the 5′- and 3′-monophosphate nucleotides, we hypothesized that substitution of a phosphate at the 5′-position of the dinucleotide would have a dramatic impact on the gas-phase conformation of the dinucleotides and thus the spatial proximity of potential deprotonated sites relative to labile hydrogen atoms. Our detailed comparison shows that much of what was previously observed for the H/D exchange of mononucleotides in a quadrupole ion trap can be extended to dinucleotides that retain similar spatial functionality. Ultimately this work is directed toward a longer term goal of understanding the gas-phase conformations and reactivity of larger oligonucleotides.

2. Experimental

2.1. Reagents

Deoxyribose dinucleotides (dAA, dAG, dGA, dGG) and 5′-monophosphate deoxyribose dinucleotides (5′P-dAA, 5′P-dAG, 5′P-dGA, 5′P-dGG) were purchased from Sigma-Genosys (The Woodlands, TX) as desalted standards. Deuterium oxide, D_2O, was purchased from Sigma–Aldrich (St. Louis, MO). All of these compounds were used without further purification. Stock standards of the dinucleotides and 5′-monophosphate dinucleotides (10^{-3} M) were prepared in water. Working standards (5.0×10^{-5} M) were prepared from the stock standards via dilution with HPLC grade methanol.

2.2. ESI-MS

A Hitachi 3DQ quadrupole ion trap mass spectrometer (model: M-8000 LC/3DQMS) equipped with an electrospray ionization (ESI) source and operated in the negative ion mode was used for all mass spectral analyses. The nitrogen sheath gas of the ESI source was set to 4.0 kg/cm^2 and the helium buffer gas inside the trap was set to 3.0 kg/cm^2, yielding a helium pressure of approximately 1 mTorr. Dinucleotide and 5′-monophosphate dinucleotide solutions were infused directly into the ESI source via a syringe pump (Harvard Apparatus, Holliston, MA) at a rate of 10 μL/min. To facilitate optimal operation of the high-flow source, an additional 120 μL/min of HPLC grade methanol was provided by a secondary pump. The adjustable temperature settings of the electrospray source were set as follows: assist gas heater 150 °C, desolvator 150 °C and aperture 150 °C. The ESI probe, drift and focus voltages were optimized at 4.0 kV, 70 V and 40 V, respectively.

2.3. H/D exchange

Gas-phase H/D exchange reactions were conducted inside the quadrupole ion trap where the typical base pressure of the system, including helium buffer gas, was nominally 5×10^{-5} Torr. Deuterium oxide, D_2O, was introduced via a custom leak valve assembly that permitted the deuterating agent to be admitted to the ion trap independent of the helium buffer gas [17]. Exchange reactions were performed at a system pressure of 3.5×10^{-4} Torr as measured by an ion gauge. Ions were accumulated for 25 ms with a subsequent isolation time of 10 ms. H/D exchange times with D_2O were then varied from an additional 10 ms to 10 s. Exchange reactions were monitored by the relative change in the abundance of

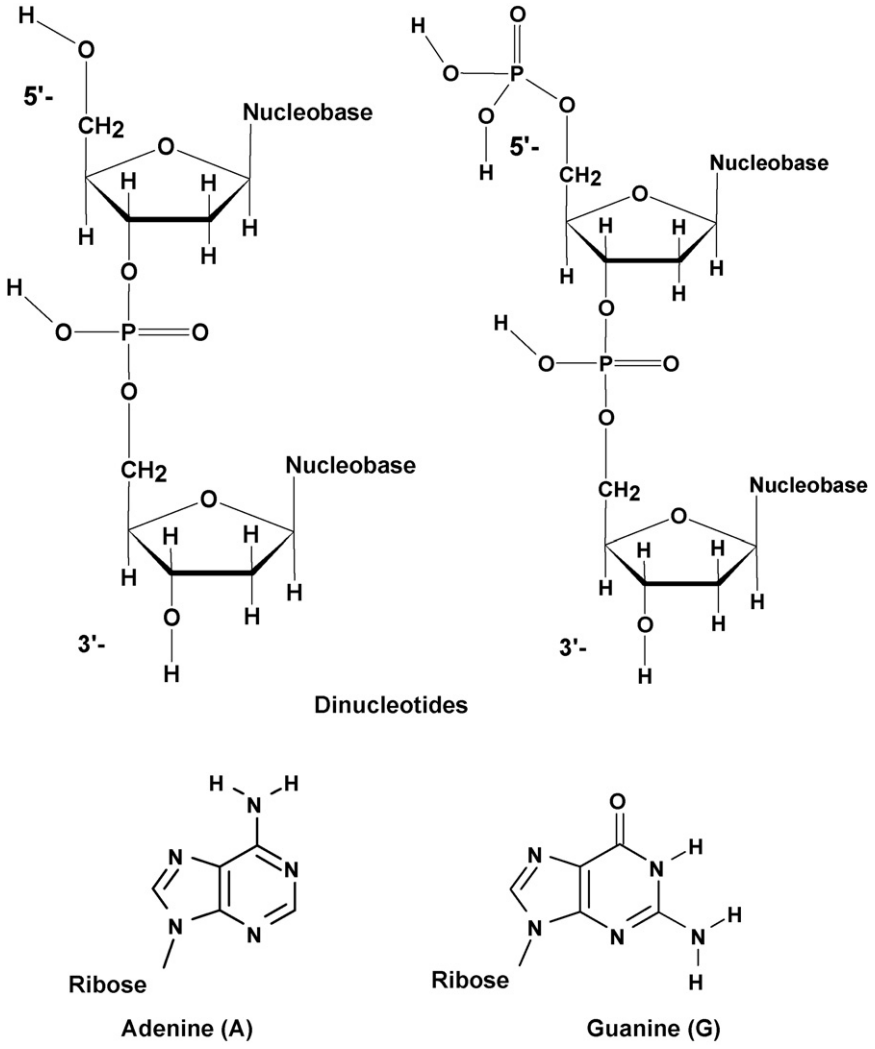

Fig. 1. Structures of the dinucleotides and the purine nucleobases adenine and guanine.

the precursor ion and deuterated species. Deuterium incorporation resulted in mass shifts designated as D(*N*), where *N* is the number of exchanged hydrogen atoms. Post-experiment isotopic corrections to exchanged peak intensities were made by subtraction of theoretical amounts of ^{13}C in each peak. Each dinucleotide and 5′-monophosphate dinucleotide was analyzed individually with the experiments being repeated on at least one other day to assess repeatability.

2.4. Molecular modeling

An extensive series of calculations were undertaken for each of the dinucleotides and 5′-monophosphate dinucleotides to facilitate the interpretation of the mass spectral data. Unless otherwise noted, all calculations were performed in the Hyperchem 7.5 modeling environment using the AMBER 99 force field. Neutral starting structures were deprotonated at the phosphate moiety to produce singly charged anions. In the case of the 5′-monophosphate dinucleotides, two different anions were created, one with the deprotonation occurring at the backbone phosphate and the other with the deprotonation occurring at the 5′-phosphorylation. Additional details about the computational modeling protocol are provided as supplementary material [34–36].

3. Results and discussion

3.1. H/D exchange mass spectra

The reactions of four deprotonated dinucleotides: [dAA-H], [dGG-H], [dGA-H] and [dAG-H]; and four analogous deprotonated 5-monophosphate dinucleotides: [5′P-dAA'-H], [5′P-dGG-H], [5′P-dGA-H] and [5′P-dAG-H], with D_2O were carried out in a quadrupole ion trap. The time allotted for the H/D exchange was varied from 10 ms to 10 s. Mass spectra that typify the results are depicted in Figs. 2 and 3, while the evolution of the reactions with time is summarized in Tables 1 and 2 and presented graphically for 5′P-dGG in Fig. 4.

Although the dinucleotides studied contained between six and eight exchangeable hydrogen atoms (i.e., those hydrogen atoms bonded to heteroatoms such as oxygen or nitrogen), the extent of the H/D exchange reactions was limited, even after 10 s of reaction time. All of the dinucleotides were observed to exchange one hydrogen for deuterium (e.g., formation of D(1)), while the reactions of dGA and dGG also produced small amounts of the doubly deuterated product, D(2), at reaction times of 5 s or greater. None of the dinucleotides were observed to exchange more than two deuterium atoms under these reaction conditions. These results generally cor-

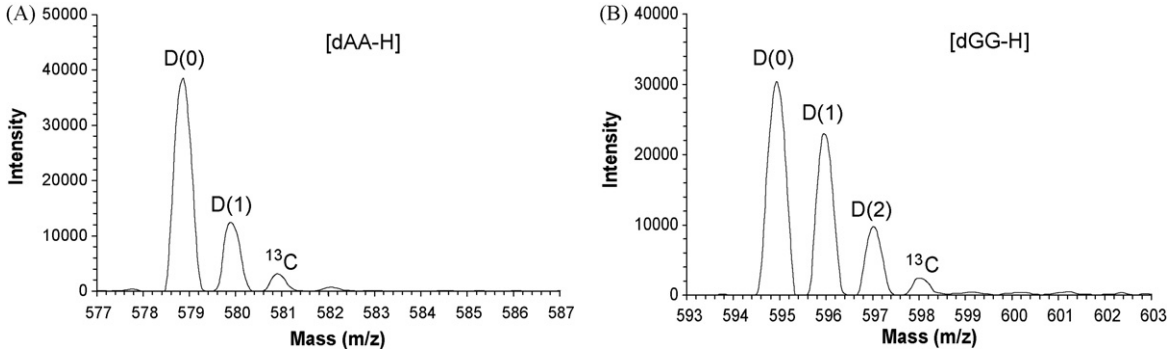

Fig. 2. H/D exchange spectra for deprotonated (A) dAA and (B) dGG after 10 s exchange with D_2O. Peaks are annotated as D(*N*) where *N* is the number of exchanged hydrogen atoms. Peaks labeled as ^{13}C can be attributed solely to the isotopic contribution of the other exchanged peaks.

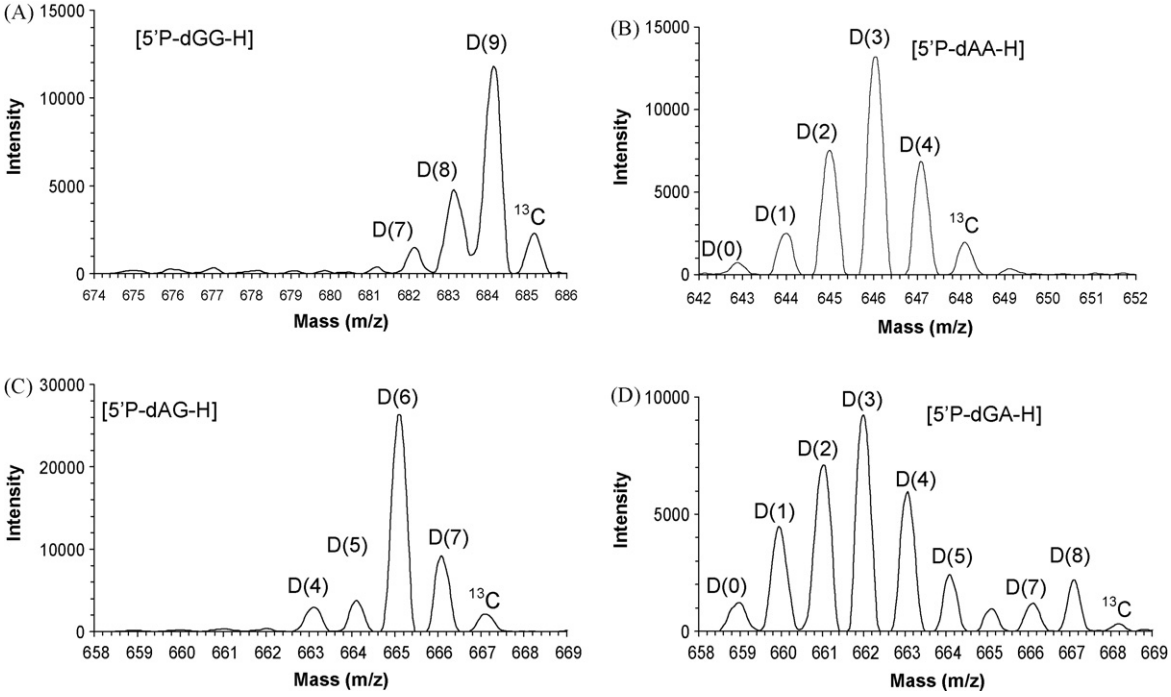

Fig. 3. H/D exchange spectra for deprotonated (A) 5′P-dGG, (B) 5′P-dAA, (C) 5′P-dAG, and (D) 5′P-dGA after 10 s exchange with D_2O. Peaks are annotated as D(*N*) where *N* is the number of exchanged hydrogen atoms. Peaks labeled as ^{13}C can be attributed solely to the isotopic contribution of the other exchanged peaks.

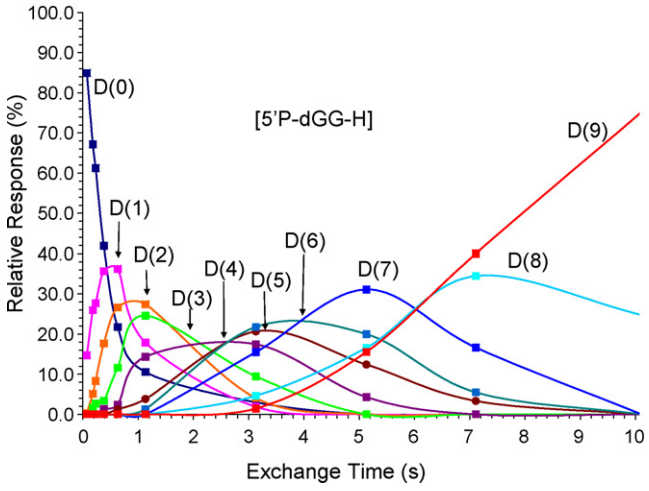

Fig. 4. Evolution of the H/D exchange reaction of deprotonated 5′P-dGG with D_2O. Curves trace the percentage of each deuterated species versus the exchange time.

relate with observations by Balbeur et al. at comparable reaction times [26], but differences in instrumentation, deuterating agent, and reagent pressures prohibit a more detailed comparison.

Although the 5′-monophosphate dinucleotides studied contained only one more exchangeable hydrogen atom than their dinucleotide counterparts (i.e., between seven and nine exchangeable hydrogen atoms), the H/D exchange reactions proceeded at both faster rates and to much greater extents. Furthermore, the identity and sequence of the nucleobases had a much larger influence on the H/D exchange for the 5′-monophosphate dinucleotides.

The H/D exchange reactions of deprotonated dGG and 5′P-dGG provide the most dramatic comparison. The former exchanged primarily one hydrogen atom, thus forming mostly D(1) and a small amount of D(2) after a reaction time of 10 s. In contrast, the analogous monophosphate compound, 5′P-dGG, completely exchanged all nine of its exchangeable hydrogen atoms, resulting in mostly D(9) with some remaining D(8) during the same time period. Clearly the addition of the 5′-monophosphate functionality encouraged an exchange process that was not accessible in the absence of the phosphorylation.

Table 1
Evolution of the H/D exchange reaction of dinucleotides with D_2O.

Dinucleotide[a]	Exchange time (s)	Percentage of dinucleotide[b,c] D(0)	D(1)	D(2)
dAA (6)	0.1	100.0	0.0	0.0
dAA (6)	1	100.0	0.0	0.0
dAA (6)	5	89.2	10.8	0.0
dAA (6)	10	86.9	13.1	0.0
dAG (7)	0.1	100.0	0.0	0.0
dAG (7)	1	97.7	2.3	0.0
dAG (7)	5	93.5	6.0	0.0
dAG (7)	10	91.0	9.0	0.0
dGA (7)	0.1	98.3	1.7	0.0
dGA (7)	1	95.8	4.2	0.0
dGA (7)	5	76.4	20.9	2.7
dGA (7)	10	64.7	31.0	4.3
dGG (8)	0.1	100.0	0.0	0.0
dGG (8)	1	93.6	6.0	0.0
dGG (8)	5	72.5	25.3	2.3
dGG (8)	10	57.8	33.9	8.4

[a] The number of exchangeable hydrogens is shown in parentheses.
[b] The percentage of each species of the dinucleotide appearing in the mass spectrum after isotopic correction for ^{13}C where D(*N*) refers to the number of incorporated deuterium atoms.
[c] RSD ±~5%.

Notable differences in the H/D exchange behavior between the dinucleotides dGA and dAG and their corresponding monophosphates, 5′P-dAG and 5′P-dGA, are also observed. As was the case with all of the dinucleotides (including not only the compounds reported here but also those containing the nucleobases cytosine and thymine), dAG and dGA exchanged primarily one hydrogen atom to form D(1) and in some instances a minor amount of D(2) after 10 s of reaction time. In contrast, both 5′P-dGA and 5′P-dAG exchanged up to seven or eight hydrogens. While this observation is noteworthy in itself, what is more striking is the differences in the exchange spectra for the two monophosphates (see Fig. 3). When the guanine nucleobase is nearest to the 3′-end of the molecule (i.e., 5′P-dAG), the H/D exchange is much more extensive, producing mostly D(6) and some D(7) at the maximum exchange time. However, when the adenine nucleobase is located in this position (i.e., 5′P-dGA) the exchange is more limited, producing mostly D(3) and D(4), and a bimodal distribution is observed. These types of bimodal distributions have been reported for the dinucleotide dTG [27] as well as longer oligonucleotides [7,27]. These results could suggest the possibility of two distinct gas-phase conformations for 5′P-dGA that did not interconvert readily, or the possibility of particular conformations exchanging via different mechanisms. These results underscore the importance of the specific sequence of the nucleobases and suggest that other isomers could also exhibit differential H/D exchange behavior.

3.2. Molecular modeling of anions and ion-molecule complexes

The analysis of the H/D exchange of the dinucleotides and 5′-monophosphate dinucleotides was enhanced by performing an extensive array of computational calculations. These calculations were designed to not only investigate the gas-phase conformations of the anions, but also to examine their interactions with the neutral D_2O molecule.

3.2.1. Conformations of gas-phase dinucleotide anions (dAA, dAG, dGA, dGG)

The annealing methodology produced both stacked and open conformations for the deprotonated dinucleotides, with the stacked conformation being lower in energy, presumably due to the stabilizing interactions of the nucleobases. Although the AMBER 99 force fields cannot account for the electronic forces associated with base stacking explicitly, calculations based on twist and base separations are in agreement with more exhaustive ab initio studies of free nucleobases [37]. Several of the conformations involved interactions between the deprotonated phosphate and the primary amino hydrogen atoms of the guanine nucleobase. In these conformations, the guanine adopted a –syn orientation over the ribose ring. This orientation has been noted in previous studies using ion-mobility and REMPI spectroscopy [30–33,38].

3.2.2. Ion-molecule complexes of dinucleotide anions (dAA, dAG, dGA, dGG)

The formation of ion-molecule complexes between neutral D_2O and representative low-energy deprotonated dinucleotide confor-

Table 2
Evolution of the H/D exchange reaction of 5′-phosphorylated dinucleotides with D_2O.

Phosphorylated dinucleotide[a]	Exchange time (s)	Percentage of phosphorylated dinucleotide[b,c] D(0)	D(1)	D(2)	D(3)	D(4)	D(5)	D(6)	D(7)	D(8)	D(9)
5′P-dAA (7)	0.1	92.6	7.4	0.0	0.0	0.0	0.0	0.0	0.0	–	–
5′P-dAA (7)	1	53.0	35.6	10.0	1.4	0.0	0.0	0.0	0.0	–	–
5′P-dAA (7)	5	8.0	24.3	37.0	29.8	0.9	0.0	0.0	0.0	–	–
5′P-dAA (7)	10	2.9	9.1	27.4	44.7	15.9	0.0	0.0	0.0	–	–
5′P-dAG (8)	0.1	54.5	33.2	10.3	2.0	0.0	0.0	0.0	0.0	0.0	–
5′P-dAG (8)	1	3.1	7.7	20.9	26.9	26.3	12.3	2.7	0.0	0.0	–
5′P-dAG (8)	5	0.0	0.0	0.0	0.0	8.3	12.5	79.1	0.0	0.0	–
5′P-dAG (8)	10	0.0	0.0	0.0	0.0	8.7	8.9	74.9	7.6	0.0	–
5′P-dGA (8)	0.1	94.1	5.9	0.0	0.0	0.0	0.0	0.0	0.0	0.0	–
5′P-dGA (8)	1	58.0	21.3	11.4	5.0	2.9	1.3	0.0	0.0	0.0	–
5′P-dGA (8)	5	16.8	30.6	28.7	10.1	2.9	1.7	4.4	4.8	0.0	–
5′P-dGA (8)	10	4.5	15.4	22.1	27.8	13.8	3.9	1.7	3.7	7.0	–
5′P-dGG (9)	0.1	67.2	26.0	5.2	1.7	0.0	0.0	0.0	0.0	0.0	0.0
5′P-dGG (9)	1	10.6	17.9	27.4	24.6	14.4	3.8	1.3	0.0	0.0	0.0
5′P-dGG (9)	5	0.0	0.0	0.0	0.0	4.3	12.4	20.0	31.1	16.6	15.6
5′P-dGG (9)	10	0.0	0.0	0.0	0.0	0.0	0.0	0.0	0.0	24.8	75.2

[a] The number of exchangeable hydrogens is shown in parentheses.
[b] The percentage of each species of the phosphorylated dinucleotide appearing in the mass spectrum after isotopic correction for ^{13}C where D(*N*) refers to the number of incorporated deuterium atoms.
[c] RSD ±~5%.

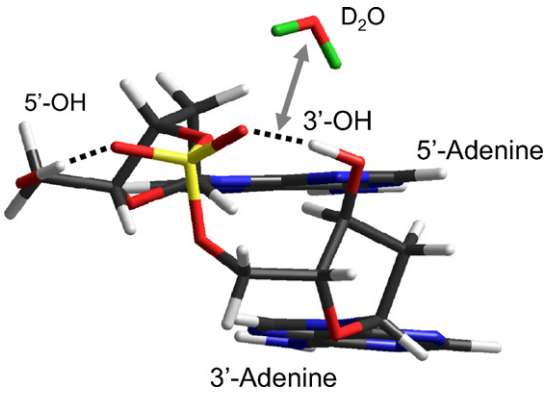

Fig. 5. The lowest energy ion-molecule complex of deprotonated dinucleotide dAA with D_2O. Deuterium atoms are depicted in green, oxygen atoms in red, hydrogen atoms in white, phosphorus atoms in yellow, nitrogen atoms in blue and carbon atoms in black. Dashed lines indicate intramolecular hydrogen bonding while gray arrows indicate ion-molecule complexation via intermolecular interaction. In this conformation the deprotonated phosphate is capable of simultaneously interacting with both the 5′- and 3′-hydroxyl groups and the D_2O molecule. The two adenine nucleobases remain remote to the deprotonation site in a stacked conformation.

mations was investigated by sequentially placing a D_2O molecule at each vertex of a three-dimensional 1 Å grid surrounding the deprotonated phosphate. The energy of the ion-molecule system was then minimized, thereby allowing the D_2O molecule to probe the anion surface in search of a local potential energy well. The array of ion-molecule complexes was subsequently sorted by relative energy and the interatomic distances between the potential relay exchange participants were measured to assess the suitability of the conformation to this type of exchange (Scheme 1).

Fig. 5 depicts the lowest energy ion-molecule complex obtained for dAA. Here, the D_2O molecule is simultaneously located within 3.0 Å of both the deprotonated phosphate and the hydrogen atom of the 3′-hydroxyl group, thereby making it amenable to exchange via the relay mechanism. This complex was typical of all of the dinucleotide anions as was a similar complex involving D_2O and the 5′-hydroxyl hydrogen atom. Furthermore, a stacked nucleobase conformation was also dominant for all of the ion-molecule complexes involving dGG and dGA, but open conformations were commonly observed for dAG. This latter observation illustrates an interesting aspect of the gas-phase conformations of any dinucleotide containing a guanine nucleobase. When a guanine was located in the 3′-position, as in dAG and dGG, rotation over the ribose ring into a –syn orientation introduced an additional hydrogen bond between a hydrogen atom of the secondary amine of guanine and the deprotonated phosphate. The calculated ion-molecule complexes with D_2O typically showed a favorable interaction at this hydrogen-bonded site. However, when the guanine was located in the 5′-position, a similar rotation facilitated a potential hydrogen bond between the 5′-hydroxyl group and a hydrogen atom of the secondary amine, but the exchangeable hydrogen atoms of the guanine nucleobase remained isolated from the deprotonated phosphate. In this case the corresponding ion-molecule complexes tended to favor interactions between the deprotonated phosphate and the 3′- or 5′-hydroxyl group. Therefore, while the H/D exchange of guanine hydrogen atoms at the 3′-end was supported by a relay mechanism, direct exchange of the same hydrogen atoms in a guanine located at the 5′-end was not. Furthermore, the formation of a hydrogen bond between the 3′-guanine and the deprotonated phosphate stabilized the open structure of dAG and at least partially offset the energy difference associated with disrupted base stacking.

As described for mononucleotide anions, adenine nucleobases favored the –*anti* orientation since rotation around the glycosidic bond that joins the nucleobase to the ribose ring did not promote any hydrogen bonding between the amino hydrogen atoms of the nucleobase and the deprotonated phosphate or the 5′-hydroxyl group [23,30]. Therefore the most favorable orientation for the adenine nucleobases was a stacked arrangement. As shown in Fig. 5, this conformation tended to seclude the adenine hydrogen atoms from the deprotonated phosphate. Correspondingly, none of the ion-molecule complexes generated for any of the dinucleotides containing adenine suggested any potential relay exchange of the associated exchangeable hydrogen atoms.

Overall, the modeling of the ion-molecule complexes formed between the dinucleotide anions and D_2O correlated well with the observed H/D exchange spectra. Exchange was predicted primarily for the exchangeable hydrogen atoms of the hydroxyl groups located at the 3′- or 5′-position. Some propensity for exchange was also observed for anions containing a guanine as the 3′-nucleobase. However, none of the computed ion-molecule complexes predicted relay exchange of any 5′-guanine nucleobase hydrogen atoms or any hydrogen atoms located on an adenine nucleobase, regardless of position. Furthermore, most of the complexes involved interaction of D_2O with only one of the exchangeable hydrogen atoms at a time. Hence it appears reasonable that the extent of H/D exchange of the dinucleotides should be limited at short timescales.

3.2.3. *Conformations of gas-phase 5-monophosphate dinucleotide anions (5′P-dAA, 5′P-dAG, 5′P-dGA, 5′P-dGG)*

Substitution of a phosphate for a hydroxyl group at the 5′-position of a dinucleotide adds both an additional exchangeable hydrogen atom and an additional site for deprotonation. Therefore, modeling of the gas-phase conformations of the 5′-monophosphate dinucleotides involved two distinct anions for each monophosphate dinucleotide, one entailing deprotonation at the phosphate that joined the two ribose rings (i.e., the conventional backbone phosphate) and one involving deprotonation at the 5′-phosphate group.

The simulated annealing results were profoundly affected by the addition of the phosphate group at the 5′-position. When the deprotonation occurred at the backbone phosphate, annealed structures tended to adopt similar conformations to those of the dinucleotides, typically with stabilizing hydrogen bonds between the deprotonated phosphate and the 3′-hydroxyl hydrogen atom. In contrast, when the deprotonation occurred at the 5′-phosphate, a richer array of low-energy conformations was generated. The additional flexibility afforded by the 5′-carbon linkage allowed the deprotonated phosphate to readily form hydrogen bonds with not only the 3′-hydroxyl hydrogen atom, but also in many cases the backbone phosphate and the labile hydrogen atoms of the nucleobases. In the deprotonated state the 5′-phosphate was often observed to disrupt the pure stacking interaction of the nucleobases that were common in the dinucleotides and thus allowed these conformations to instead distort into hydrogen-bonded nucleobase structures. Fig. 6 depicts one illustration of this phenomenon for 5′P-dAG, whose corresponding dinucleotide favored either stacked or primarily open conformations, but not hydrogen-bonded ones.

3.2.4. *Ion-molecule complexes of 5-monophosphate dinucleotide anions (5′P-dAA, 5′P-dAG, 5′P-dGA, 5′P-dGG)*

The additional distribution of gas-phase conformations generated for the 5′-monophosphate dinucleotides also translated to a wider array of conformations amenable to ion-molecule complexation and subsequent H/D exchange via a relay mechanism. Fig. 7 depicts one such example for the 5′-monophosphate dinucleotide, 5′P-dGG. In this case the stacking interactions of the two guanine

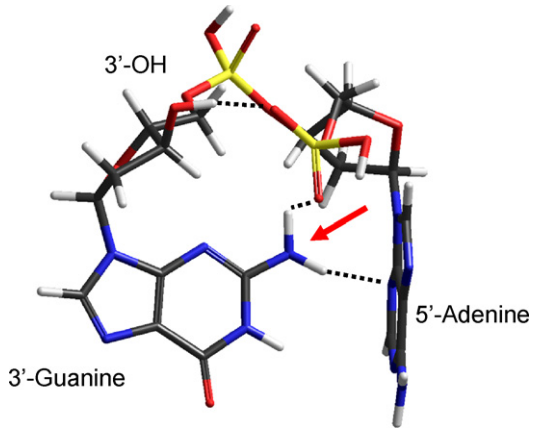

Fig. 6. The lowest energy conformation of deprotonated 5′-monophosphate dinucleotide 5′P-dAG. Oxygen atoms are depicted in red, hydrogen atoms in white, phosphorus atoms in yellow, nitrogen atoms in blue and carbon atoms in black. Dashed lines indicate intramolecular hydrogen bonding while the red arrows emphasizes the position of the amino group of the 3′-guanine. The presence of the deprotonated 5′-phosphate facilitates the formation of a hydrogen bond between the two nucleobases by providing additional stabilization between the phosphate and the 3′-guanine. These conformations were not observed in the corresponding dinucleotide, dAG.

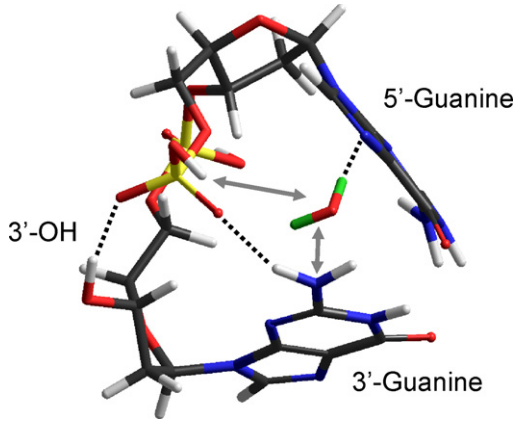

Fig. 7. The lowest energy ion-molecule complex of deprotonated 5′-monophosphate dinucleotide 5′P-dGG with D_2O. Deuterium atoms are depicted in green, oxygen atoms in red, hydrogen atoms in white, phosphorus atoms in yellow, nitrogen atoms in blue and carbon atoms in black. Dashed lines indicate intramolecular hydrogen bonding while gray arrows indicate ion-molecule complexation via intermolecular interaction. The nucleobases remain in a distorted stacked position with the flexible 5′-deprotonated phosphate bound to both the 3′-hydroxyl group and the 3′-amino atoms of guanine. The D_2O molecule is within 3 Å of the exchangeable hydrogen atoms of guanine and the 5′-phosphate.

nucleobases are distorted by the presence of the deprotonated 5′-phosphate. The D_2O molecule contributes to the stabilization of this complex by hydrogen bonding to a nitrogen atom of the 5′-guanine and positioning itself within 3 Å of both the deprotonated phosphate and the secondary amino hydrogen atoms of the 3′-guanine. This type of complex was unique to the 5′-phosphorylated dinucleotides and not observed in the analogous dinucleotides. Exchange of the labile hydrogen atoms of the 3′-guanine nucleobase

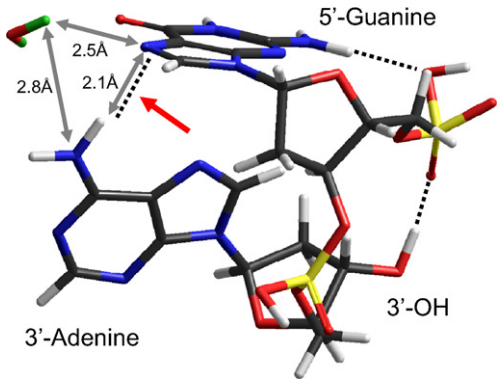

Fig. 8. A low-energy ion-molecule complex of deprotonated 5′-monophosphate dinucleotide 5′P-dGA with D_2O. Deuterium atoms are depicted in green, oxygen atoms in red, hydrogen atoms in white, phosphorus atoms in yellow, nitrogen atoms in blue and carbon atoms in black. Dashed lines indicate intramolecular hydrogen bonding. Hydrogen bonding between the nucleobases (red arrow) could facilitate a shuttling mechanism that results in exchange of the 3′-adenine hydrogen atoms (gray arrows).

is thus a favored process for 5′P-dAG and 5′P-dGG, which could explain the much larger extent of exchange for these compounds compared to those with an adenine at the 3′-end (Fig. 3).

As evident from the mass spectra in Fig. 3, the sequence of the nucleobases in the 5′-monophosphate dinucleotides 5′P-dGA and 5′P-dAG had a distinct effect on the observed H/D exchange spectra. The interactions of the deprotonated 5′-monophosphate with the nucleobases in the low-energy ion-molecule complexes of these two oligonucleotides illustrates the importance of their gas-phase conformations on the H/D exchange behavior. Both of these anions favored the formation of hydrogen-bonded complexes; however the presence of the guanine nucleotide at the 3′-end of 5′P-dAG allowed the 5′-phosphate to interact with both the 5′-adenine and 3′-guanine in a bound conformation. In contrast, positioning of the adenine at the 3′-position, furthest from the deprotonated phosphate, tended to exclude those labile hydrogen atoms and instead favored interaction of the deprotonation site with the 5′-guanine and 3′-hydroxyl groups. Thus, it is likely a combination of the orientation of the guanine nucleobase relative to the ribose ring and the ability of the deprotonated phosphate to stabilize or discourage stacking of the nucleobases which results in the dramatic differences in H/D exchange spectra of these two isomeric oligonucleotides.

While a relay mechanism appears to correlate with the majority of the H/D exchange observed for these dinucleotides and 5′-monophosphate dinucleotides, it cannot completely explain the extensive exchange recently reported for some of these compounds via lengthy reactions in an FT-ICR [26], nor the apparent bimodal distribution observed here for 5′P-dGA. Other gas-phase exchange mechanisms have been proposed, each supposing specific steric, energetic, thermodynamic, or kinetic conditions on the exchange reaction [2,3,14]. Of particular interest in this case are mechanisms that involve direct interaction of the deuterating agent with the exchangeable hydrogen atoms. Two examples are the kinetic mechanism recently reported by Balbeur et al. [26] and the flip-

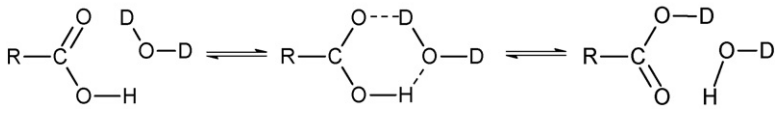

Scheme 2. H/D exchange via a flip-flop mechanism. The reaction is shown for a generic carboxylic acid reacting with deuterated oxide (D_2O).

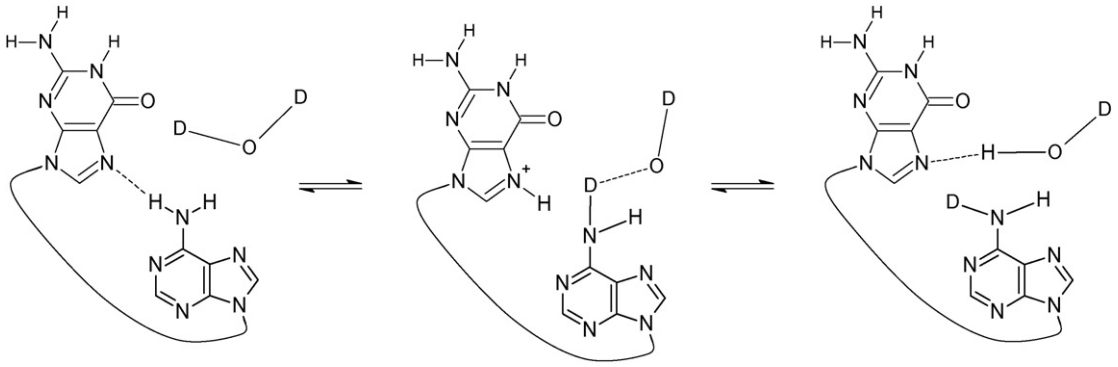

Scheme 3. H/D exchange via a shuttling mechanism. The reaction is initiated by hydrogen bonding between the two nucleobases in conjunction with complexation by the deuterating agent. Exchange proceeds via shuttling of the hydrogen and deuterium atoms among the acidic deuterating agent and two basic nucleobases. Unlike the relay mechanism, H/D exchange may occur remote from the deprotonation site.

flop mechanism first reported by Campbell et al. [14] and later investigated with peptides [19,21] and dicarboxylic acids [24] by others. While the kinetic mechanism was proposed in an effort to explain extremely fast, simultaneous exchanges, the flip-flop mechanism has been shown to proceed at a much slower rate than relay exchange [19,21,24].

A typical flip-flop mechanism contains a six- or eight-membered pseudo ring structure formed by the attraction of two partially charged participants, and exchange occurs as one of the potential outcomes of its disassembly (Scheme 2). Fig. 8 depicts a similar type arrangement for the 5′P-dGA anion in which hydrogen bonding between the 5′-guanine and 3′-adenine in concert with additional interactions with an acidic D_2O molecule creates a complex where hydrogen and deuterium atoms may be shuttled amongst hydrogen bonds formed by the participants. As shown in Scheme 3, complexes adopting this unique conformation may effectively result in H/D exchange of some of the 3′-adenine labile hydrogen atoms. The ion-molecule complex depicted in Fig. 8 is of similar energy (∼+2 kcal/mole) to the lowest energy complex formed between 5′P-dGA anions and D_2O. The only structural difference between the two complexes is the location of the D_2O molecule. In the lowest energy complex, the D_2O interacts with the deprotonation site and the secondary amino hydrogen atoms of the 5′-guanine instead of the two hydrogen-bonded nucleobases. The extent to which the conformation in Fig. 8 impacts the observed H/D exchange depends on the formation of the ion-molecule complex, its stability, and the kinetics of the hydrogen/deuterium shuttling.

Ultimately, the proposed shuttling mechanism is similar to both the relay and flip-flop mechanisms. Like the relay mechanism, the deuterating agent in the shuttling mechanism interacts with two distant groups of the ion. However, in this case the two nucleobases are also hydrogen bonded and the deuterating agent is not the sole "bridge" between the two groups. More importantly, the shuttling mechanism does not require the proximity of the deprotonation site to the labile hydrogen atoms for H/D exchange to occur. H/D exchange remote from the deprotonation site is a distinguishing characteristic of the flip-flop mechanism. However, the shuttling mechanism is slightly different from the flip-flop mechanism in that H/D exchange does not occur directly with the amine functionality of the 3′-adenine, but instead requires the participation of the 5′-guanine via hydrogen bonding to the 3′-adenine. No additional high-level ab initio calculations or specific studies of model compounds were performed to further explore this shuttling mechanism. However, if it were to occur, it could explain the additional H/D exchange of the 3′-adenine labile hydrogen atoms for which the relay mechanism fails to account. Future efforts will explore this hypothesis more extensively.

4. Conclusions

Remarkable differences were noted in the gas-phase hydrogen/deuterium (H/D) exchange reactions of D_2O with four deprotonated dinucleotides (dAA, dAG, dGA, dGG) and their analogous 5′-monophosphates (5′-dAA, 5′-dAG, 5′-dGA, 5′-dGG). For the dinucleotides, H/D exchange was limited, even at the maximum reaction time. Computational investigations of the gas-phase conformations of these anions and their ion-molecule complexes suggested that few of the exchangeable hydrogen atoms were amenable to exchange via the relay mechanism. Instead, those located on the nucleobase tended to remain remote from the deprotonation site as stacking interactions stabilized many of the dinucleotide conformations and precluded a favorable spatial relationship of the deprotonation site and labile hydrogen atoms.

The proclivity for H/D exchange of the analogous 5′-monophosphates was not only dramatically increased, but also shown to be both nucleobase- and sequence-dependent. The associated computations revealed a more impressive array of low-energy conformations, including many "bound" conformations where the deprotonated 5′-phosphate partially disrupted the normal stacking interaction, but compensated energetically by forming additional hydrogen bonds to the nucleobases. Ion-molecule complexes formed by these and other conformations showed a much larger tendency for interaction between the deprotonation site and the exchangeable hydrogen atoms of not only the 3′-hydroxyl group, but also many of the labile hydrogen atoms of the nucleobases. Together the experimental and computational results support the feasibility of a relay mechanism for H/D exchange in oligonucleotides. However, the relay mechanism may not adequately explain all of the observed H/D exchange. Certainly other mechanisms such as the flip-flop, onium, zwitterionic, scrambling and recently proposed kinetic mechanism exist and several may be acting in concert to produce the observed H/D exchange. A new shuttling mechanism that functions via a three member hydrogen-bonded complex may also be one of these.

Acknowledgements

Funding from the Welch Foundation (F1155) and the NIH (RO1 GM65956) is gratefully acknowledged. In addition, the authors

would like to thank Junmei Wang for his assistance with the RESP calculations and NCSA for the computational time.

Appendix A. Supplementary data

Supplementary data associated with this article can be found, in the online version, at doi:10.1016/j.ijms.2008.09.011.

References

[1] J.J. Grabowski, C.H. DePuy, J.M. Van Doren, V.M. Bierbaum, J. Am. Chem. Soc. 107 (1985) 7384.
[2] E. Gard, M.K. Grenn, J. Bregar, C.B. Lebrilla, J. Am. Soc. Mass Spectrom. 5 (1994) 623.
[3] S.C. Campbell, M.T. Rodgers, E.M. Marzluff, J.L. Beauchamp, J. Am. Chem. Soc. 117 (1995) 12840.
[4] J.M. Robinson, M.J. Greig, R.H. Griffey, M. Venkantraman, D.A. Laude, Anal. Chem. 70 (1998) 3566.
[5] M.A. Freitas, S.D.-H. Shi, C.L. Hendrickson, A.G. Marshall, J. Am. Chem. Soc. 120 (1998) 10187.
[6] G.E. Reid, R.J. Simpson, R.A.J. O'Hair, Int. J. Mass Spectrom. 191 (1999) 209.
[7] R.H. Griffey, M.J. Grieg, J.M. Robinson, D.A. Laude, Rapid Commun. Mass Spectrom. 13 (1999) 113.
[8] T. Felix, M. Reyzer, J. Brodbelt, Int. J. Mass Spectrom. 191 (1999) 161.
[9] M.L. Reyzer, J.S. Brodbelt, J. Am. Soc. Mass Spectrom. 11 (2000) 711.
[10] T.G. Schaaff, J.L. Stephenson Jr., S.A. McLuckey, J. Am. Soc. Mass Spectrom. 11 (2000) 167.
[11] S.A. Hofstadler, K.A. Sannes-Lowery, R.H. Griffey, J. Mass Spectrom. 35 (2000) 62.
[12] M.A. Freitas, A.G. Marshall, J. Am. Soc. Mass Spectrom. 12 (2001) 780.
[13] K.B. Green-Church, P.A. Limbach, M.A. Freitas, A.G. Marshall, J. Am. Soc. Mass Spectrom. 12 (2001) 268.
[14] D. Reed, S.R. Kass, J. Am. Soc. Mass Spectrom. 12 (2001) 1163.
[15] M.E. Crestoni, S.J. Fornarini, J. Mass Spectrom. 38 (2003) 854.
[16] T. Wyttenbach, B. Paizs, P. Barran, L. Breci, D. Liu, S. Suhai, V.H. Wysocki, M.T. Bowers, J. Am. Chem. Soc. 125 (2003) 13768.
[17] J. Zhang, J.S. Brodbelt, J. Am. Chem. Soc. 126 (2004) 5906.
[18] K. Hermann, V. Wysocki, E. Vorpagel, J. Am. Soc. Mass Spectrom. 16 (2005) 1067.
[19] M. Rožman, J. Am. Soc. Mass Spectrom. 16 (2005) 1846.
[20] V. Gabelica, F. Rosu, M. Witt, G. Baykut, E. De Pauw, Rapid Commun. Mass Spectrom. 19 (2005) 201.
[21] M. Rožman, B. Bertoša, L. Klasinc, D. Srzić, J. Am. Soc. Mass Spectrom. 17 (2006) 29.
[22] K.A. Hermann, K. Kuppannan, V.H. Wysocki, Int. J. Mass Spectrom. 249–250 (2006) 93.
[23] J.E. Chipuk, J.S. Brodbelt, J. Am. Soc. Mass Spectrom. 18 (2007) 724.
[24] J.E. Chipuk, J.S. Brodbelt, Int. J. Mass Spectrom. 267 (2007) 98.
[25] J. Mo, K. Håkansson, Anal. Chem. 79 (2007) 7893.
[26] D. Balbeur, D. Dehareng, E. De Pauw, J. Am. Soc. Mass Spectrom. 18 (2007) 1827.
[27] D. Balbeur, J. Widart, B. Leyh, L. Cravello, E. De Pauw, J. Am. Soc. Mass Spectrom. 19 (2008) 938.
[28] D. Mao, K.R. Babu, Y.L. Chen, D.J. Douglas, Anal. Chem. 75 (2003) 1325.
[29] F.W. McLafferty, Z. Guan, U. Haupts, T.D. Wood, N.L. Kelleher, J. Am. Chem. Soc. 120 (1998) 4732.
[30] J. Gidden, M.T. Bowers, J. Phys. Chem. 107 (2003) 12829.
[31] J. Gidden, J.E. Bushnell, M.T. Bowers, J. Am. Chem. Soc. 123 (2001) 5610.
[32] J. Gidden, M.T. Bowers, Eur. Phys. J. D 20 (2002) 409.
[33] T. Wyttenbach, M.T. Bowers, J. Am. Soc. Mass Spectrom. 10 (1999) 9.
[34] J. Wang, W. Wang, P.A. Kollman, D.A. Case, J. Mol. Graph. Modell. 25 (2006) 247.
[35] J. Wang, R.M. Wolf, J. Caldwell, P.A. Kollman, D.A. Case, J. Comp. Chem. 25 (2004) 1157.
[36] M.J. Frisch, G.W. Trucks, H.B. Schlegel, G.E. Scuseria, M.A. Robb, J.R. Cheeseman, J.A. Montgomery Jr., T. Vreven, K.N. Kudin, J.C. Burant, J.M. Millam, S.S. Iyengar, J. Tomasi, V. Barone, B. Mennucci, M. Cossi, G. Scalmani, N. Rega, G.A. Petersson, H. Nakatsuji, M. Hada, M. Ehara, K. Toyota, R. Fukuda, J. Hasegawa, M. Ishida, T. Nakajima, Y. Honda, O. Kitao, H. Nakai, M. Klene, X. Li, J.E. Knox, H.P. Hratchian, J.B. Cross, C. Adamo, J. Jaramillo, R. Gomperts, R.E. Stratmann, O. Yazyev, A.J. Austin, R. Cammi, C. Pomelli, J.W. Ochterski, P.Y. Ayala, K. Morokuma, G.A. Voth, P. Salvador, J.J. Dannenberg, V.G. Zakrzewski, S. Dapprich, A.D. Daniels, M.C. Strain, O. Farkas, D.K. Malick, A.D. Rabuck, K. Raghavachari, J.B. Foresman, J.V. Ortiz, Q.A. Cui, G. Baboul, S. Clifford, J. Cioslowski, B.B. Stefanov, G. Liu, A. Liashenko, P. Piskorz, I. Komaromi, R.L. Martin, D.J. Fox, T. Keith, M.A. Al-Laham, C.Y. Peng, A. Nanayakkara, M. Challacombe, P.M.W. Gill, B. Johnson, W. Chen, M.W. Wong, C. Gonzalez, J.A. Pople, Gaussian 03, Revision C.02, Gaussian Inc., Wallingford, CT, 2004.
[37] P. Hobza, M. Kabelac, J. Sponer, P. Mejzlik, J. Vondrasek, J. Comp. Chem 18 (1997) 1136.
[38] X. Yang, X. Wang, E.R. Vorpagel, L. Wang, Proc. Natl. Acad. Sci. U.S.A. 101 (2004) 17588.